0.0.1 Parton distributions at large x

Knowledge of parton distributions forms the basis of our understanding of matter in term of fundamental constituents. However, extracting parton distributions in the large x domain is notoriously difficult. For polarized parton distributions, the problem comes from the lower available luminosity and from staying away from partonic initial and final state interactions. This imposes Q^2 greater than a few GeV^2 and W greater than a few GeV in addition to the large x constraint. In the unpolarized case, luminosities are adequate and free proton targets exist, so proton data are satisfactory. For the neutron no such targets exist and deuteron is used. The difficulty is to control sufficiently well nuclear final state interactions (FSI) and binding effects to allow for a systematically accurate extraction of the neutron information.

The consequence of these difficulties can be readily seen on Figure 1. The lack of experimental constraints allows for a variety of predictions that needs to be sorted out to establish the right phenomenology. Studies of parton distributions have already been undertaken at JLab, with $x \leq 0.6$. The BoNuS experiment [1], gathered neutron data that emanates from quasi-free neutrons within unpolarized deuterons. The FSI and binding effects were minimized by measuring recoiling protons and selecting events for which the two nucleons were not interacting. On the polarized data front, data were collected up to $x \sim 0.6$ in Halls A and B [2, 3]. An exciting outcome is the failure of leading order (LO) pQCD to describe the data, hinting that the validity domain of LO pQCD is not reached yet or that quark orbital momentum (an important but experimentally elusive contribution to the nucleon spin) may be sizable. The mismatch between LO pQCD prediction and experimental data can be best seen on the ratio of polarized d quark distribution over the unpolarized one, see Fig. 2.

A 11 GeV beam allows measurements up to $x \sim 0.8$. The luminosity expected with unpolarized gaseous deuterium target needed for the recoil proton tagging method is 5×10^{35} cm^{-2}s^{-1}. It is about 10^{35} cm^{-2}s^{-1} for the polarized target currently under design. Those and the large solid angle of CLAS12 makes it a superior choice to measure parton distributions at large x, sort out mechanisms of SU(6) symmetry breaking and of quark-hadron duality and explore the role of quark orbital momentum. In addition, to their intrinsic interest, quark distributions at large x are crucial for estimating backgrounds in searches for physics beyond the Standard Model at high energy colliders [6].

To Extend the BoNuS results to higher x, a proposal [4] for 35 days of running at 11 GeV was submitted to JLab PAC30 and conditionally approved. The experiment will use the standard CLAS12 equipment with the additional recoil detector already used in E03-012 [1]. The anticipated results can be seen in Fig. 3 for F_2^n/F_2^p (left) and u/d (right). Clearly the F_2^n/F_2^p data obtained using the new method will allow us to differentiate unambiguously between different expectations for this ratio.

JLab PAC30 also approved E12-06-109 [5] which will, in particular, study polarized parton distributions at large x. Using standard detection equipment, a redesigned polarized target adapted to CLAS12 and 30 (50) days of running on longitudinally

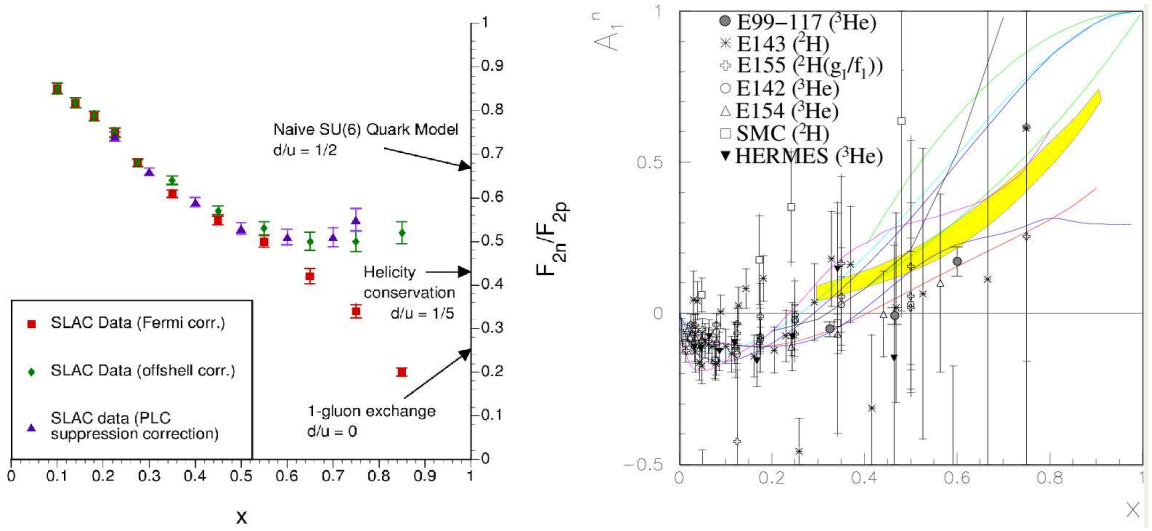

Figure 1: World data on the d/u parton distribution ratio from unpolarized measurements of F_2^n/F_2^p (left) and on the photon asymmetry A_1^n from polarized data (right). The substantial systematic (left) or statistic (right) errors at large x do not permit to constrain the various predictions.

polarized NH_3 (ND_3) target, high precision measurements can be achieved as shown in Fig. 4. These data will disentangle models in the large-x. While the results shown in Fig. 4 are with a $W > 2$ constraint, hadron-parton duality studies (see page 8) will tell us by how much this constraint can be relaxed, possibly increasing the x range up to 0.9. The expected accuracy for $(\Delta d + \Delta\bar{d})/(d + \bar{d})$ is shown on Fig. 5.

0.0.2 Global fit of polarized parton distributions

The large window opened by the 12 GeV upgrade over the DIS domain will permit to constrain global fits of parton distributions. The unique impact at large x has

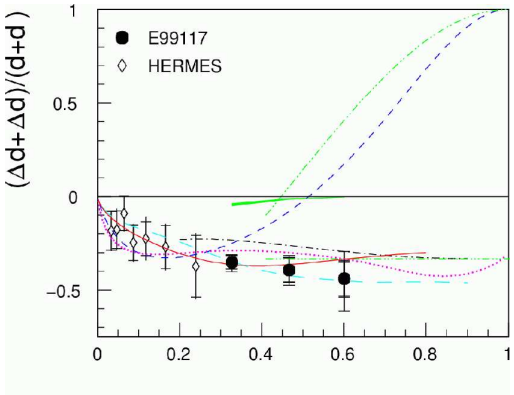

Figure 2: $(\Delta d + \Delta\bar{d})/(d + \bar{d})$as extracted from $A1$ [2]. The leading order pQCD predictions is given by the dashed curve.

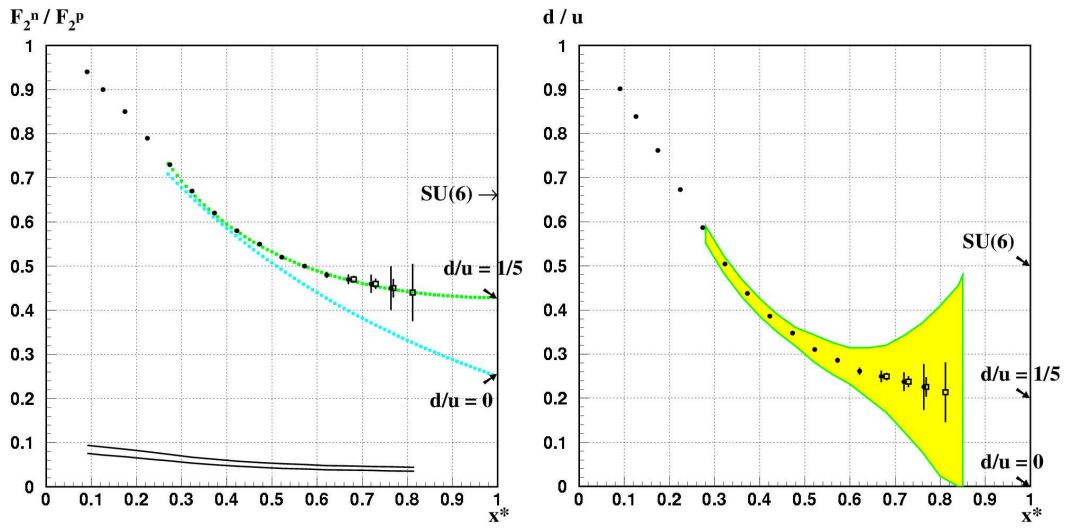

Figure 3: Anticipated results on F_2^n/F_2^p (left) and the subsequent u/d ratio (right) for 35 days of data taking at 11 GeV. The arrows along the ordinate indicate model predictions. The error bars pertaining to filled circles are statistical with a $W > 2$ GeV constrain. The smaller errors (with open squares) are for $W > 1.8$ GeV. The systematic error is indicated by the higher band along the abscissa on the left plot. Point to point correlated errors can be suppressed by normalizing the low x points to existing data, giving a point to point uncorrelated systematic error represented by the lower band. The two curves on the left plot represent hadron-parton duality based predictions with two different mechanisms for SU(6) symmetry breaking. The shaded band on the right plot indicates our present knowledge on the d/u ratio.

just been discussed. The improvement from the 12 GeV upgrade is also significant at low and moderate x, noticeably for the polarized gluon distribution ΔG. For a more complete picture of the precision achievable with the expected CLAS12 data, we have plotted in Fig. 6 an analysis of the impact on NLO analyzes. A dramatic improvement can be achieved with the expected data from the CLAS12 proposal E12-060109 [5]. We emphasize that the data will not only reduce the error band on ΔG but will likely allow a more detailed modeling of its x-dependence.

0.0.3 Moments of structure functions

Moments of structure functions provide powerful insight into the underlying structure of nucleons. Recent inclusive data at Jefferson Lab permitted us to evaluate some of these moments at low and intermediate Q^2 [10, 11]. With a maximum beam energy of 6 GeV, however, the measured strength of the moments becomes rather limited for Q^2 greater than a few GeV^2. The 12 GeV upgrade will remove this problem and allow for measurements to higher Q^2.

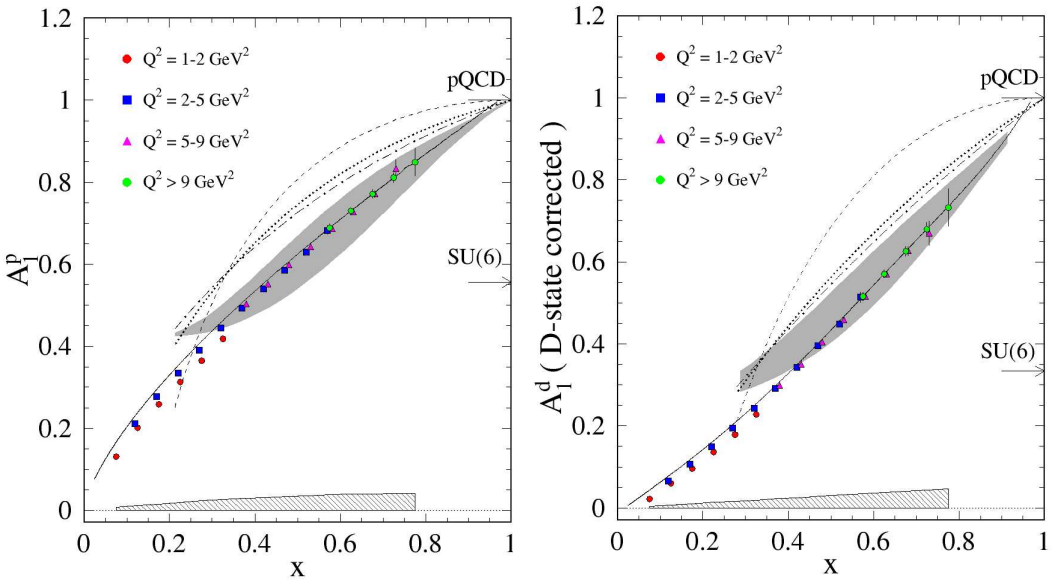

Figure 4: Anticipated results on A_1^p (left) and A_1^d (right). The four different symbols represent four different Q^2 ranges. The statistical uncertainty is given by the error bars while the systematic uncertainty is given by the shaded band.

Moments of spin structure function can be related to static properties of the nucleon by sum rules. At large Q^2 the Bjorken Sum Rule relates the difference of g_1 for the proton and the neutron to the axial coupling constant [12]. At the other end of the spectrum, $Q^2 = 0$, the Gerasimov-Drell-Hearn (GDH) Sum Rule links the difference of spin dependent cross sections, integrated over the photon energy, to the anomalous magnetic moment of the nucleon [13]. These two sum rules are aspects of a more general one derived recently by Ji and Osborne [14] that is valid at any Q^2 and links the first moments of spin structure functions to spin-dependent Compton amplitudes. Low Q^2 is an excellent testing ground for chiral perturbation theory calculations, while moments measured at large Q^2 can be compared to Higher Twist series derived within the operator product expansion (OPE) method. Lattice QCD can calculate higher twist terms, thus extending the domain of applicability of OPE to lower Q^2. However OPE is unusable at low Q^2. To bridge the gap, lattice QCD can be used to compute spin-dependent Compton amplitudes at any Q^2. Hence, the Ji and Osborne sum rule can be computed and compared to experiments at any Q^2. It offers an unique opportunity to study the transition from partonic to hadronic degrees of freedom.

The left plot on Fig. 7 shows the expected precision on the measured part of Γ_1^p. The inner error bar is statistical while the outer one is the statistical and systematical uncertainties added in quadrature. Published results and preliminary results from EG1b are also displayed for comparison. Like the CLAS12 data, the EG1 data do not include the unmeasured DIS contribution. The hatched blue band corresponds

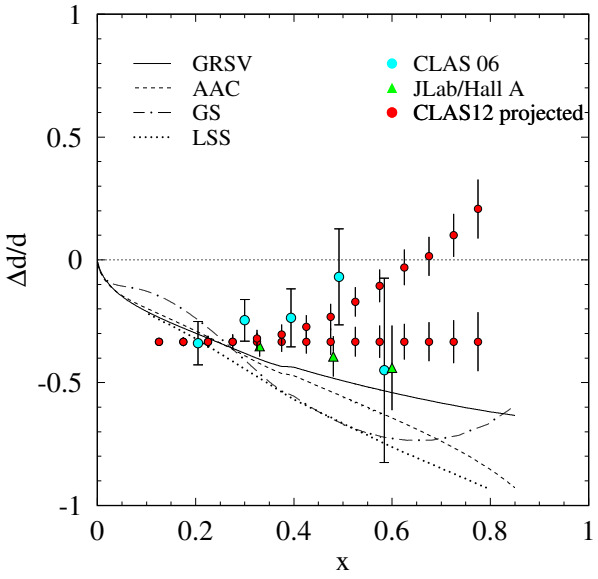

Figure 5: Expected result for $(\Delta d + \Delta\bar{d})/(d + \bar{d})$. The central values of the data are following two arbitrary curves to demonstrate how the two categories of predictions, namely the ones that predict $\Delta d/d$ to stay negative (LO and NLO analyzes of polarized DIS data: GRSV, LSS, AAC, GS, statistical model and a quark-hadron duality scenario) and the ones predicting $\Delta d/d \to 1$ when $x \to 1$ (Leading order pQCD and a quark-hadron duality scenario)

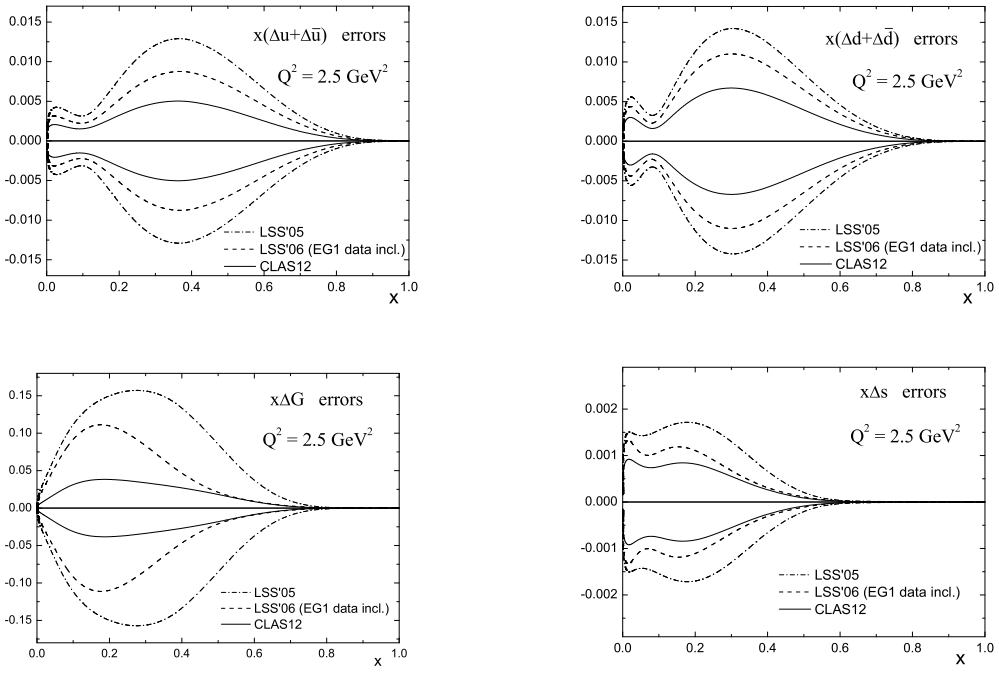

Figure 6: Expected uncertainties for Δu, Δd, ΔG and Δs from a NLO analysis of all world data. The outermost line shows the result from the analysis by Leader, Sidorov and Stamenov [8].The second line is the updated result after inclusion of the new EG1b data from CLAS at 5.7 GeV [9]. The innermost line shows the expected uncertainty after including the data set to be collected with CLAS12, including statistical and systematic errors.

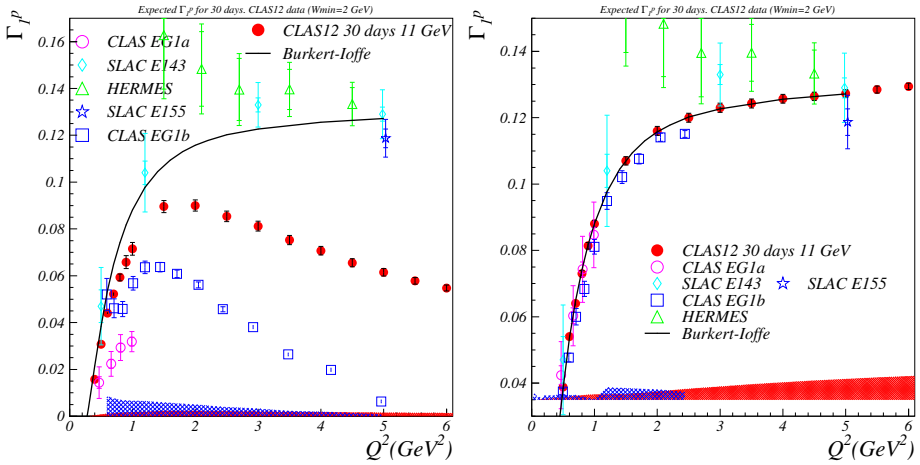

Figure 7: Left plot: expected precision on Γ_1^p for CLAS12 and 30 days of running. CLAS EG1a [10] data and preliminary results from EG1b are shown for comparison. The data and systematic uncertainties do not include estimates of the unmeasured DIS contribution. HERMES [15] data and SLAC E143 [16] and E155 data [17] are also shown. These data include DIS contribution estimates. The model is from Burkert and Ioffe [18]. Right plot: same as left but including an estimate of the DIS contribution.

to the systematic uncertainty on the EG1b data points. The red band indicates the estimated systematic uncertainty from CLAS12. The right plot on Fig. 7 shows the results on Γ_1^p and Γ_1^d including an estimate of the unmeasured DIS contribution. The systematic uncertainties for EG1 and CLAS12 here include the estimated uncertainty on the unmeasured DIS part estimated using the model from Bianchi and Thomas [19]. As can be seen, moments can be measured up to $Q^2 = 6$ GeV^2 with a statistical accuracy improved several fold over that of the existing world data.

Higher moments are also of interest: generalized spin polarizabilities are linked to higher moments of spin structure functions by sum rules based on similar grounds as the GDH sum rule. Higher moments are less sensitive to the unmeasured low-x part so measurements are possible up to higher Q^2 compared to first moments. Just like the GDH/Bjorken sum rules, measurements of the Q^2-evolution allow us to study the parton-hadron transition since theoretical predictions exist at low and large Q^2 [11]. In addition, spin polarizabilities are also fundamental observables characterizing the nucleon structure and the only practical way known to measure them is through measurement of moments and application of the corresponding sum rules.

Finally, moments in the low ($\simeq 0.5$ GeV^2) to moderate ($\simeq$4 GeV^2) Q^2-range enable us to extract higher twist parameters. Those are correlations between quarks in the nucleon. This extraction can be done by studying the Q^2 evolution of first moments [11]. Higher twists have been consistently found to have, overall, a surprisingly

smaller effect than expected. Going to lower Q^2 enhances the higher twist effects but makes it harder to disentangle a high twist from the yet higher ones. Furthermore the uncertainty on α_s becomes prohibitive at low Q^2. Hence, higher twists turn out to be hard to measure, even at the present JLab energies. Adding higher Q^2 to the present JLab data set removes the issues of disentangling higher twists from each others and of the α_s uncertainty. The smallness of higher twists, however, requires a statistically precise measurements with small point to point correlated systematic uncertainties. Such precision at moderate Q^2 has not been achieved by the experiments done at high energy accelerators, while JLab at 12 GeV presents the opportunity to reach it. Using the expected statistic and systematic uncertainties of E012-06-109 and the same procedure as in Ref. [20]. The total Bjorken sum, f_2^{p-n}, decreases by a factor 5.6 compared to results obtained in [20].

The GDH Sum Rule Despite its fundamental nature, the GDH sum rule has not yet been fully verified experimentally. Combined results from MAMI and ELSA [32] are about 10% above the expected value. This is for upper integration limit of a photon energy of about 2.8 GeV. With the cancellation of the fixed target program at SLAC and consequently of the experiment E159 [33] that would have investigated the GDH strength at large ν, Jefferson Lab is now the best place to test the convergence of the GDH sum. Using real photons or near real photons, we can measure the contribution to the GDH Sum Rule up to 10.5 GeV, about 4 times the maximum energy reached at ELSA, see figure 8. A non convergence of the sum rule would be intriguing and may signal physics beyond the standard model. In any case it will provide important insight on soft Regge physics.

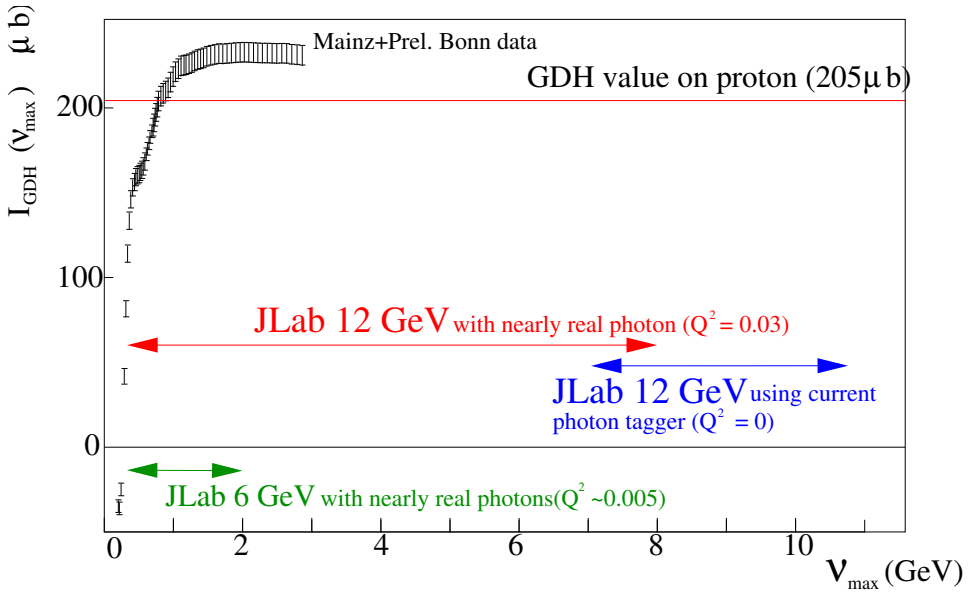

Figure 8: Coverage for low-Q^2 experiment with CLAS and CLAS12. The data points are the GDH running sum from MAMI and ELSA at $Q^2 = 0$.

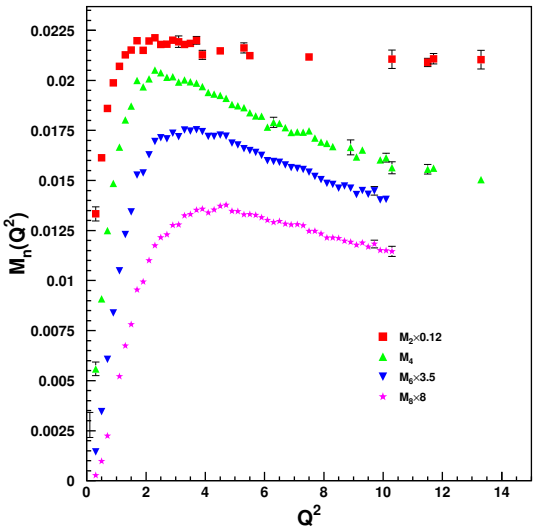

Figure 9: Expected moments of the proton structure function F_2 obtained with the CLAS12 detector simulations for a few days of running. The meaning of the markers and the scale factors for each moment are indicated in the inset.

Moments of the structure function F_2 and precise determination of $\alpha_s(M_Z)$ Simulated results for the moments $\int_0^1 dx x^n F_2$ with $n \leq 8$ are reported in Fig. 9. It shows that CLAS12 will provide a unique tool to extract moments of the structure function F_2 up to $10 \div 14$ $(\mathrm{GeV/c})^2$. These can be used to extract the strong coupling constant $\alpha_s(M_z)$. The extraction of $\alpha_s(M_Z)$ from the scaling violations of the proton structure function F_2 is one of the most precise methods available up to now (see Fig. 10). Simulation shows that a new procedure for the extraction of $\alpha_s(M_Z)$ Ref. [30] together with the CLAS12 data can allow a unprecedentedly accurate determination of $\alpha_s(M_Z)$ with a statistical uncertainty of 0.0008 and a systematic uncertainty of about 0.0007.

Quark-hadron duality The phenomenon of quark-hadron duality relates the physics of nucleon resonances to the dynamics of single quark scattering which governs the scaling structure functions at high energy. Measurements [24, 28] at Jefferson Lab of the unpolarized proton structure functions in the resonance region have sparked considerable interest in quark-hadron duality [23, 34, 35]. While quark-hadron duality has been observed in the spin-independent F_2 structure function [23, 24], it has not yet been firmly established for spin-dependent structure functions. Because the g_1 structure function is given by a difference of cross sections, which need not be positive, the workings of duality will necessarily be more intricate for g_1 than for the spin-averaged F_2 structure function. The first results from the spin structure function measurements in Hall A [25, 27] and Hall B [26] indicate that, if one averages over the entire resonance region, duality roughly holds for Q^2 above 1.5 GeV^2. To achieve a more precise understanding of the mechanism of duality it is necessary to determine the conditions under which duality occurs in both polarized and unpolarized structure functions. An upgraded CLAS12 would permit to measuring structure functions in the DIS region high precision. For unpolarized parton distribution, the tagging

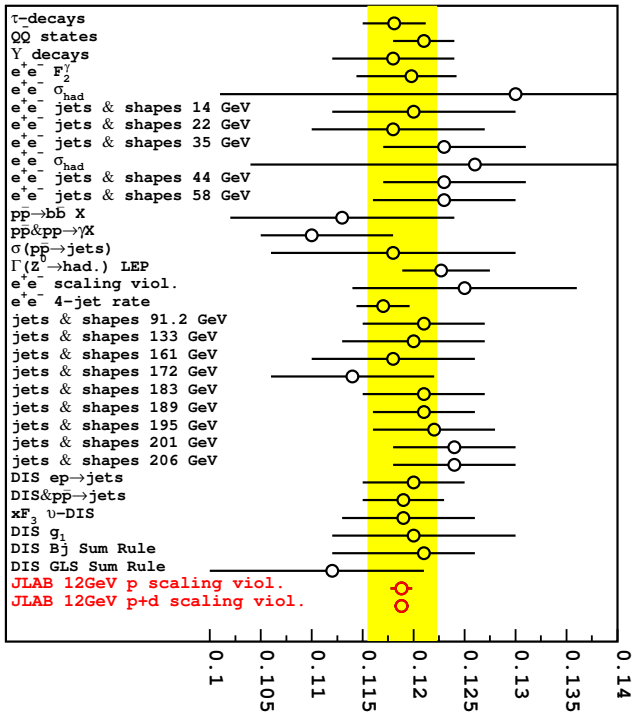

Figure 10: Existing determinations of the QCD coupling constant $\alpha_S(M_Z)$ [31].

technique used by the BoNuS experiment [1] and described in section 0.0.1 can also be applied to the neutron resonance region, where at present there are essentially no data.

Bibliography

[1] JLab E03-12, The Structure of the Free Neutron Via Spectator Tagging. H. Fenker, C. Keppe, S. Kuhn and W. Melnitchouk spokespersons.

[2] X. Zheng *et al.*, Phys. Rev. Lett. **92**, 012004 (2004); Phys. Rev. **C70** 065207 (2004).

[3] K.V. Dharmawardane *et al.*, Phys.Lett. **B641** 11 (2006).

[4] JLab E12-06-113, The Structure of the Free Neutron at Large x-Bjorken. S. Bueltmann, M. Christy, H. Fenker, K. Griffioen, C. Keppel, S. Kuhn, W. Melnitchouk, V. Tvaskis spokespersons.

[5] E12-06-109 The Longitudinal Spin Structure of the Nucleon. D. Crabb, A. Deur, K. Dharmawardane, T. Forest, K. Griffioen, M. Holtrop, S. Kuhn, Y. Prok

[6] S. Kuhlmann *et al.*, Phys. Lett. B **476**, 291 (2000).

[7] W. Melnitchouk and A. W. Thomas, Phys. Lett. B **377**, 11 (1996).

[8] E. Leader, A. V. Sidorov and D. B. Stamenov, Phys. Rev. D **73**, 034023 (2006) [arXiv:hep-ph/0512114].

[9] K. V. Dharmawardane, S. E. Kuhn, P. Bosted and Y. Prok [the CLAS Collaboration], to be published in Phys. Lett., arXiv:nucl-ex/0605028.

[10] R. Fatemi *et al.* [CLAS Collaboration], Phys. Rev. Lett. **91**, 222002 (2003), J. Yun *et al.* [CLAS Collaboration], Phys. Rev. C **67**, 055204 (2003).

[11] J.-P. Chen, A. Deur, Z.-E. Meziani, Mod. Phys. Lett. **A20**, 2745 (2005); M. Osipenko *et al.*, Phys. Rev. D **71**, 054007 (2005).

[12] J. D. Bjorken, Phys. Rev. **148**, 1467 (1966).

[13] S. D. Drell and A. C. Hearn, Phys. Rev. Lett. **16**, 908 (1966); S. Gerasimov, Sov. J. Nucl. Phys. **2**, 430 (1966).

[14] X. Ji and J. Osborne, J. Phys. **G27** 127 (2001).

[15] HERMES collaboration: A. Airapetian *et al.*, Eur. Phys. J. **C26**, 527 (2003).

[16] E143 collaboration: K. Abe *et al.*, Phys. Rev. Lett. **78**, 815 (1997); K. Abe *et al.*, Phys. Rev. D **58**, 112003 (1998).

[17] P.L. Anthony *et al.,* Phys. Lett. **B493**, 19 (2000).

[18] V. D. Burkert and B. L. Ioffe, Phys. Lett. **B296**, 223 (1992); J. Exp. Theor. Phys. **78**, 619 (1994).

[19] N. Bianchi and E. Thomas, Nucl. Phys. Proc. Suppl. **82**, 256 (2000).

[20] A. Deur *et al.*, Phys. Rev. Lett. **93** 212001 (2004)

[21] J.P. Chen, A. Deur and F. Garibaldi, JLab experiment E97-110

[22] M. Battaglieri, A. Deur, R. De Vita and M. Ripani, JLab experiment E03-006

[23] E. D. Bloom and F. J. Gilman, Phys. Rev. Lett. **16**, 1140 (1970); Phys. Rev. D **4**, 2901 (1971).

[24] I. Niculescu *et al.*, Phys. Rev. Lett. **85**, 1182, 1186 (2000).

[25] M. Amarian *et al.*, Phys. Rev. Lett. **92** 022301 (2004)

[26] P.E. Bosted *et al.*, hep-ph/0607283

[27] P. Solvigon, Contribution to the proceedings of the First Workshop on Quark-Hadron Duality and the Transition to pQCD. A. Fantoni, S. Luiti and O. Rondon ed. World Scientific, 2006.

[28] M. E. Christy *et al.*, E94-110 Collaboration, in preparation.

[29] M. Osipenko *et al.*, Phys. Rev. **D67** 09201 (2003)

[30] S. Simula and M. Osipenko, Nucl. Phys. **B675** 289 (2003)

[31] S. Bethke, α_S 2002 High-Energy Physics Int'l Conference in Quantum Chromodynamics, Montpellier (France) (2002)

[32] K. Helbing. Talk given at the GDH04 symposium. www.physics.odu.edu/GDH2004/Proceedings/Helbing.pdf

[33] SLAC experiment E159. P. Bosted and D. Crabb spokespersons. www.slac.stanford.edu/exp/e159/prop.pdf

[34] A. de Rújula, H. Georgi and H. D. Politzer, Ann. Phys. **103**, 315 (1975).

[35] N. Isgur, S. Jeschonnek, W. Melnitchouk and J. W. Van Orden, Phys. Rev. D **65**, 054005 (2001).